
**Separation Science and Technology**
Publication details, including instructions for authors and subscription information:
http://www.informaworld.com/smpp/title~content=t713708471

# Removal of Micron-Size Droplets from an Air Stream by Means of Electric Fields

C. K. Riahi-Nezhad[a]; C. Tsouris[a]; D. W. DePaoli[a]; V. F. de Almeida[a]
[a] Nuclear Science and Technology Division, Oak Ridge National Laboratory, Oak Ridge, TN, USA

**To cite this Article** Riahi-Nezhad, C. K. , Tsouris, C. , DePaoli, D. W. and de Almeida, V. F.(2005) 'Removal of Micron-Size Droplets from an Air Stream by Means of Electric Fields', Separation Science and Technology, 40: 1, 367 — 381
**To link to this Article: DOI:** 10.1081/SS-200042463
**URL:** http://dx.doi.org/10.1081/SS-200042463

*Separation Science and Technology*, 40: 367–381, 2005
ISSN 0149-6395 print/1520-5754 online
DOI: 10.1081/SS-200042463



# Removal of Micron-Size Droplets from an Air Stream by Means of Electric Fields

**C. K. Riahi-Nezhad, C. Tsouris, D. W. DePaoli, and V. F. de Almeida**
Nuclear Science and Technology Division, Oak Ridge National Laboratory, Oak Ridge, TN, USA

**Abstract:** In many tank retrieval and waste treatment operations conducted for the U.S. Department of Energy, small droplets of aqueous solutions containing radioactive materials are formed in air streams. These droplets need to be separated before the air is released to the environment. The use of an electric field to separate water droplets from an air stream has been investigated. A test chamber of 10 × 10 cm cross-section and approximately 94 cm long mounted vertically was set up without packing, with two parallel-plate steel electrodes facing each other at a distance of 8 cm. An air stream containing water droplets formed by ultrasonic humidifiers was forced through the chamber. A laser-light-scattering particle-sizing system was used to measure the droplet size distribution. The droplet removal efficiency increased approximately linearly with electric field strength over the range investigated except when the field was raised to 3.0 to 3.50 kV/cm, suggesting a saturation effect. The analysis showed that the removal efficiency is a function of the initial droplet concentration. For instance, for a droplet concentration of 24.2 $g/m^3$, the maximum removal efficiency was approximately 85%, while that for a concentration of 8.3 $g/m^3$ was 65% under the same experimental conditions. Droplet size measurements revealed that the average size of droplets did not change significantly with voltage; however, the number distribution of drops did change. Appreciable changes in the number of droplets were



Funding for this research was provided by the Environmental Management Science Program and the Office of Basic Energy Sciences, Office of Chemical Sciences, U.S. Department of Energy, under contract DE-AC05-00OR22725 with UT-Battelle, LLC. The authors are also grateful to Drs. Jack S. Watson and George C. Frazier for their invaluable suggestions during the work.

Address correspondence to C. Tsouris, Nuclear Science and Technology Division, Oak Ridge National Laboratory, Oak Ridge, TN 37831-6181, USA. E-mail: tsourisc@ornl.gov

observed for droplet sizes in a typical range of 4 to 10 μm. The results of this research may be useful in developing effective applications of electric fields for the elimination of mist from air or gaseous streams.

## INTRODUCTION

The growing concern regarding the production of radioactive aerosols during treatment and sludge retrieval operations in high-level radioactive waste tanks has led the U.S. Department of Energy (DOE) to an increasing interest in reducing the emissions, worker exposure, cost, and increased waste volume from such tanks.

It should be emphasized that the human exposure to hazardous aerosol particles, in general, and submicron particles, in particular, has been a major health concern over the past decade. Submicron particles (including droplets) constitute the most serious environmental- and health-related problems. One problem is that such small particles are able to penetrate into the human lung system, where the exchange of gases between blood and air takes place (1). The human lower pulmonary system is unfortunately very efficient in retaining particles in the 1 μm range (2, 3). The deposition of small particles in the pulmonary system tends to intensify such respiratory diseases as bronchitis, emphysema, and lung cancer (3). In addition, submicron particles will stay in the atmosphere for a considerable period of time, scattering the sunlight and dissipating over a large area (4).

It is known that the removal of small particles from process or waste streams is costly and often very time consuming (5). Elimination of liquid droplets and/or solid particles from gas or vapor streams is a common operation in a variety of chemical and environmental processes. Typical mist eliminators are designed to operate as coalescers or agglomerators and thereby form larger droplets that can be removed from the process by gravity or shear forces. Droplets of a size smaller than 10 μm are, in general, difficult to remove from gaseous streams. Current particle-removing techniques (cyclone, electrostatic precipitator, scrubbers, etc.) have been used to remove larger droplets/particles from a carrier gas with high efficiency (6). The effect of electric fields on particle agglomeration has been investigated by Loffler and Gutsch (7) and Zhang et al. (8), while Luckner et al. (9) have studied electric-field bed filtration. An electrically driven process, including mechanisms such as electrocoalescence and electrophoresis, is employed in this research, with the objective to remove fine droplets from a gaseous stream.

Granular filtration (deep-bed filtration) is mechanically simple and consumes little energy. However, it relies principally on the mechanisms of interception, sedimentation, diffusion, inertia, and surface forces, which yield low collision efficiency between particles and collectors (10). It is well known that the efficiency of aerosol filtration in fiber mats (11) and in granular beds

(12) can be improved by the application of an electric field to the filter media. A filtration efficiency greater than 99% has been reported in the literature (13).

In addition, several reports on investigations of electrically enhanced aerosol filtration in fiber filters have been published (11, 14–16). Successful mathematical analyses of electrified fiber filtration have also been presented (17, 18).

The primary aim of this research is to investigate drop coalescence and demonstrate the effectiveness of electric fields in the removal of fine aerosol droplets in the absence of packing materials such as those in filters. The overall experience and knowledge gained will be useful in developing effective applications of superimposed electric fields for the elimination of mist from air or gaseous streams. Experimental studies have been undertaken for enhancing the agglomeration of small droplets by means of direct current (dc) electric fields. Measurements have been conducted in order to accomplish the following tasks: (a) quantify removal of drops by an electric field and (b) measure drop size distribution along the flow chamber and determine the effect of an electric field on drop coalescence.



## EXPERIMENTAL SETUP AND METHODS

The experimental setup for this study is shown schematically in Figs. 1 and 2. The aerosol observation chamber unit was designed to allow application of a

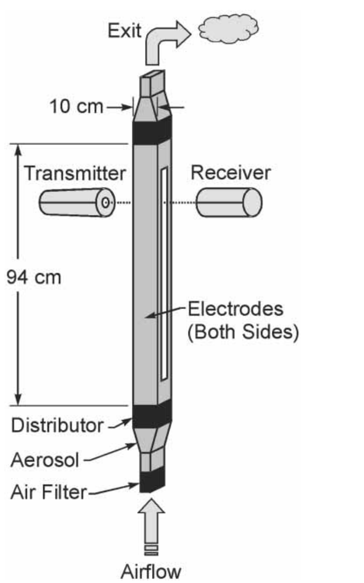


***Figure 1.*** Diagram of electrocoalescence unit system.

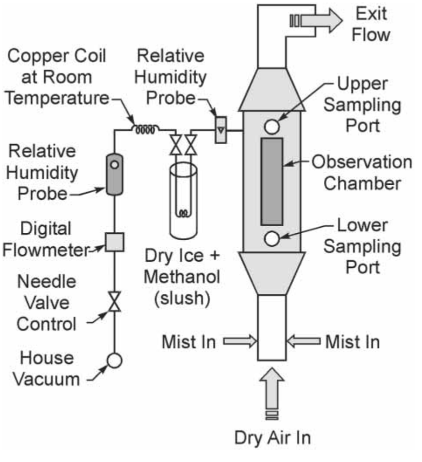


*Figure 2.* Schematic diagram of experimental setup.



relatively strong electric field. The chamber unit is made of clear Lexan with a cross-sectional area of $10 \times 10$ cm and approximately 94 cm long. On opposite sides of test windows, two 9- $\times$ 60-cm steel electrodes are mounted vertically inside the chamber. The rectangular test view window is made of flat optical glass (nonreflecting) of dimensions $2 \times 60$ cm (Fig. 1). A heating tape was attached to the glass to keep its temperature slightly above ambient to prevent accumulation of moisture during operation. A high voltage of up to 28 kV was applied to the positive electrode during the experiment by a dc power supply; the other electrode was connected to ground.

The top section of the chamber is connected by flexible ductwork to the exhaust in a hood. Two sampling ports are available on the test section of the chamber. At the bottom of the tunnel, mist from two ultrasonic humidifiers was introduced into the air stream by a diffuser (as shown in Fig. 2). The bottom part of the test section was connected to the steel duct, which was heated before each experiment to prevent condensation. Supplied house air was passed through a flow meter and an air filter before delivering the mist through the test section of the chamber. At the entrance of the test section, a honeycomb baffle was placed for constant and evenly distributed airflow. It should be noted that distilled water was used for the two ultrasonic humidifiers (Electro-Tech System, Model 5612) that generated the aerosol flowing through the test chamber.

A probe was used to measure the relative humidity/temperature of flowing air at the exit of the test section. The concentration of water droplets in the gas stream was determined by condensation of droplets from an isokinetically collected sample stream. The flow rate of the sampling stream was set such that the velocity at the sampling line entrance was equal to the average velocity in the chamber. In addition, the copper sampling probe was heated to evaporate the deposited water droplets at the edge of and inside the probe. To capture the water droplets using an isokinetic sampling probe, a slush of dry ice and methanol was prepared in a Dewar flask. During sampling, a controlled flow rate of gas was pulled out by house vacuum through a copper coil (2.0 m long and 1.25 cm ID) immersed in the slush. The copper coil was weighed before and after sampling using a sensitive balance (Metter PJ 3600 Delta Range). A battery-powered relative humidity/temperature probe (ALNOR APM-360) was used to monitor the inlet and exit relative humidity for mass balance calculations. A pressure device (SENSOTEC SC Series) was also connected to the relative humidity/temperature probe chamber to monitor the pressure drop in the dry-ice system. The details of calculations of droplet concentration are described by Riahi-Nezhad (19).



### Particle Size Distribution Measurements

The aerosol size distribution in the test chamber is determined by laser light scattering using a Malvern Spraytec RTS 5006 droplet sizing system, which is mounted on a movable stage for measurements at various heights along the column. The particle-sensing region or sample-volume forward direction is collected by the receiver lens and focused onto an annular ring detector. More details about the RTS 5006 particle size analyzer are provided by Riahi-Nezhad (19).

Before drop size distribution measurements were recorded in each run, the reference noise and then the background measurements were obtained. The background is a measure of stray light in the optical system and, most importantly, particulate contamination of the windows. The computer continuously records and saves drop size distribution data. Variables such as light transmission, particle diameter (μm) vs. cumulative volume (%), and volume frequency (%) for each run are also continuously recorded.

## RESULTS AND DISCUSSION

Prior to the discussion of experimental results, it is important to point out the following observations:

- At zero voltage, the mist distribution was uniform throughout the test chamber.

- At a given voltage level, the water droplets were deposited first on the lower end of the positive electrode. As the experiment progressed over time, droplet accumulation was observed to progress up the surfaces of both electrodes. Droplets drained down the electrodes and pooled on the bottom of the test unit.
- The electric field caused the mist motion to change from a uniform to a non-uniform pattern with motion toward the positive electrode. This fluctuating droplet motion toward the electrodes was especially intense in the voltage range of 20 kV and above.
- In all cases, at high voltages, droplet buildup at the lower level of the test chamber caused a short circuit between the positive and negative electrodes, resulting in sparks and thereby automatically shutting down the electric field for safety reasons. It was therefore necessary to limit the voltage drop across the electrodes to 26 kV to avoid electrical arcing in the test apparatus.



## Test Conditions

All experimental measurements were obtained at room temperature of approximately 23°C and ambient pressure of 750 mm Hg. The air density ($\rho_{air} = 1.19\,\mathrm{kg/m^3}$), air dynamic viscosity ($\mu_{air} = 1.86 \times 10^{-5}\,\mathrm{kg/m \cdot s}$), and duct equivalent diameter ($D_e = 0.115\,\mathrm{m}$) were assumed for the calculation of Reynolds number in all experiments. The accuracy of the dry-ice trap method was tested by measuring the mass of water vapor in the air passed through the trap and using a material balance equation. The mass of water from the room air collected in the trap and that calculated by using the material balance (assuming an ideal gas) were compared; the error was found to be within 6%. This range was confirmed for different flow rates used in the experiments (Table 1).

***Table 1.*** Percent error of measured and calculated mass of collected water from room air at variable flow rates

| Run | Flow rate (L/min) | Measured mass (g) | Calculated mass (g) | Percent error |
|---|---|---|---|---|
| 1 | 3.0 | 0.38 | 0.40 | 5.00 |
| 2 | 4.5 | 0.50 | 0.53 | 5.66 |
| 3 | 5.0 | 0.58 | 0.62 | 6.50 |
| 4 | 5.5 | 0.48 | 0.50 | 4.00 |
| 5 | 6.0 | 0.50 | 0.53 | 5.70 |
| 6 | 7.0 | 0.63 | 0.65 | 3.08 |

Each experimental run was made at a fixed value of the airflow rate and mist flow rate. The range of Reynolds number was from 940 to 2400 in all experiments. The mist concentration and light transmission were measured for each experiment at applied voltages of 0, 10, 15, 18, 20, 22, 24, and 26 kV. These values were selected based on the power supply and the test chamber limitations.

## Effects of Electric Field Strength on Droplet Concentration

Figure 3 shows experimental data obtained by the isokinetic/dry-ice sampling method at a Reynolds number of 1350. The standard deviation for all experimental data is shown in the form of error bars. The figure indicates that as the applied electric potential increases, the quantity of the mist in the air stream decreases. This is due to the increasing number of collisions between droplets (agglomeration), between droplets and electrodes, and between droplets and the chamber walls as the droplets flow in the tunnel under the influence of the electric field.

## Effects of Electric Field Strength on Light Transmission

Figure 4 shows the relationship between the concentration of collected droplets and light transmission. Examination of each individual data point



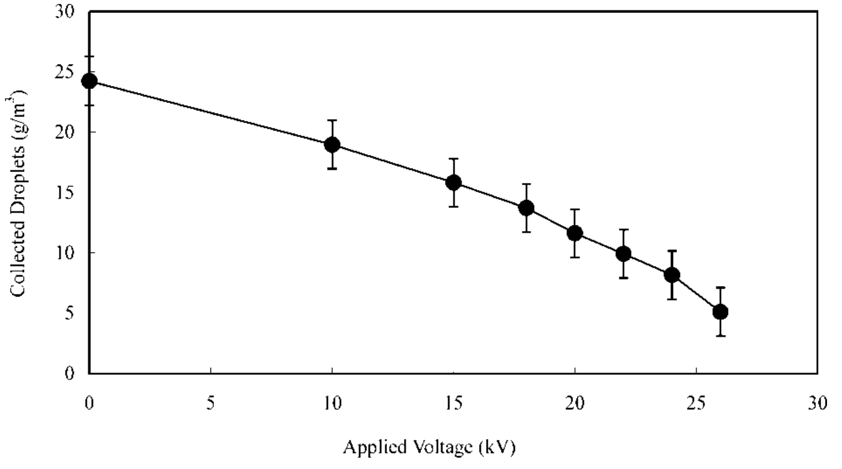


***Figure 3.*** Droplet concentration vs. applied voltage at a Reynolds number of 1350.

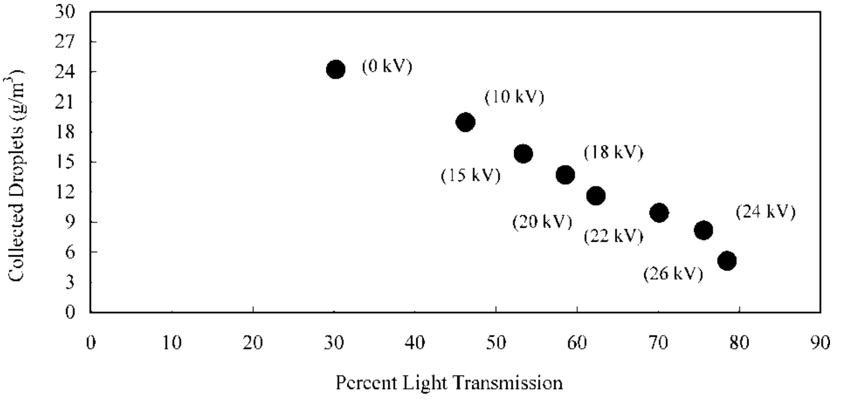


***Figure 4.*** Droplet concentration vs. percent light transmission at Reynolds number of 1350 under varying applied voltage.



reveals that the light transmission is related directly to mist concentration and can be used for estimating droplet concentration.

## Effect of Electric Field on Droplet Number

A number of experiments were conducted to quantify the effect of electric field on both average droplet size and droplet size distribution. The average droplet size ($d_{ave}$) was calculated by averaging all sizes of droplets that passed through the laser path. The number of droplets was determined in the following manner:

- Determine the average droplet volume, $V_{ave} = 4\pi/3\ (d_{ave}/2)^3$.
- Measure the mist density obtained via the dry-ice method.
- Multiply the volume frequency obtained from the light-scattering instrument by the mist density to determine the total water volume fraction, $V_x$, for each discrete droplet size.
- Estimate the number of droplets by dividing $V_x$ by $V_{ave}$.

Figure 5 shows the distributions of number of droplets vs. the average droplet size at Reynolds number 1620 and inlet mist concentration of 12.4 ($g/m^3$) for a range of applied voltages. The figure reveals that the size range of droplets does not change significantly with voltage; however, the distribution of the number of droplets does change. The changes are rather significant for droplet sizes in the range of 4 to 8 μm. For instance, when the applied voltage increases from 0 to 22 kV, the number of droplets decreases from

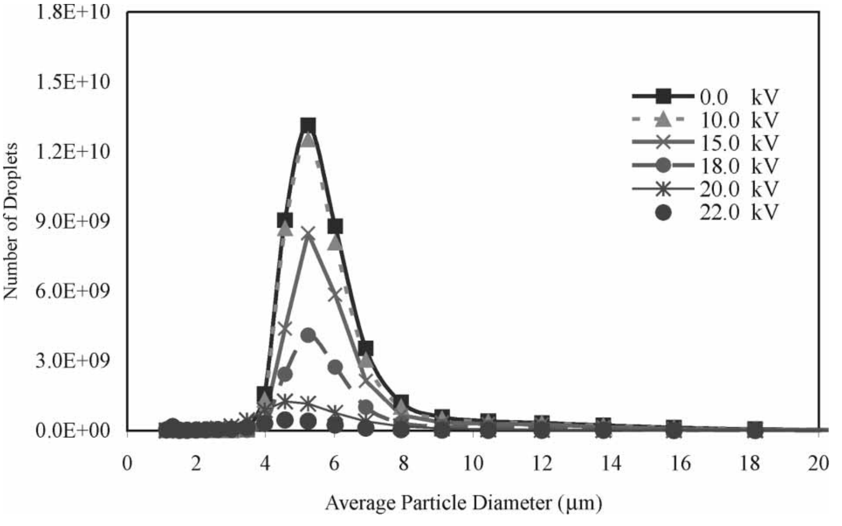


***Figure 5.*** Number of droplets vs. particle diameter at inlet mist concentration of 12.4 $g/m^3$ and Reynolds number of 1620.



$1.3 \times 10^{10}$ to $4.0 \times 10^{8}$ for the droplet size 5.23 μm. This large reduction is attributed to the collision of droplets with the electrodes and the test chamber walls. As a result of these collisions, many droplets attach to the chamber wall and electrodes and eventually flow downward to the chamber floor.

## Size Distribution Measurements

A number of experiments were conducted to determine whether the size of droplets could vary as the Reynolds number and mist concentration change under different voltage levels. In one experiment, the airflow rate was arbitrarily changed to a specific value corresponding to a Reynolds number of 1230. At this number, the measured droplet concentration from the dry-ice trap method was 12.1 ($g/m^3$) for a zero voltage.

The droplet size distributions for 0 and 26 kV are shown in Figs. 6a and 6b. A comparison of the two figures indicates that the size distribution range is increased from 3.97 to 31.56 μm to 3.97 to 47.78 μm. It also reveals that the light transmission is increased from 63.5 to 94.4%. The reason for these differences could be the enhanced agglomeration and droplet removal at higher voltages. The droplet size is a bimodal distribution, which is expected for agglomerating systems. In droplet size distribution measurements, we have observed bimodal distributions, even at 0 V. This implies that agglomeration of droplets occurs due to shear flow in delivery lines and in the input stream.

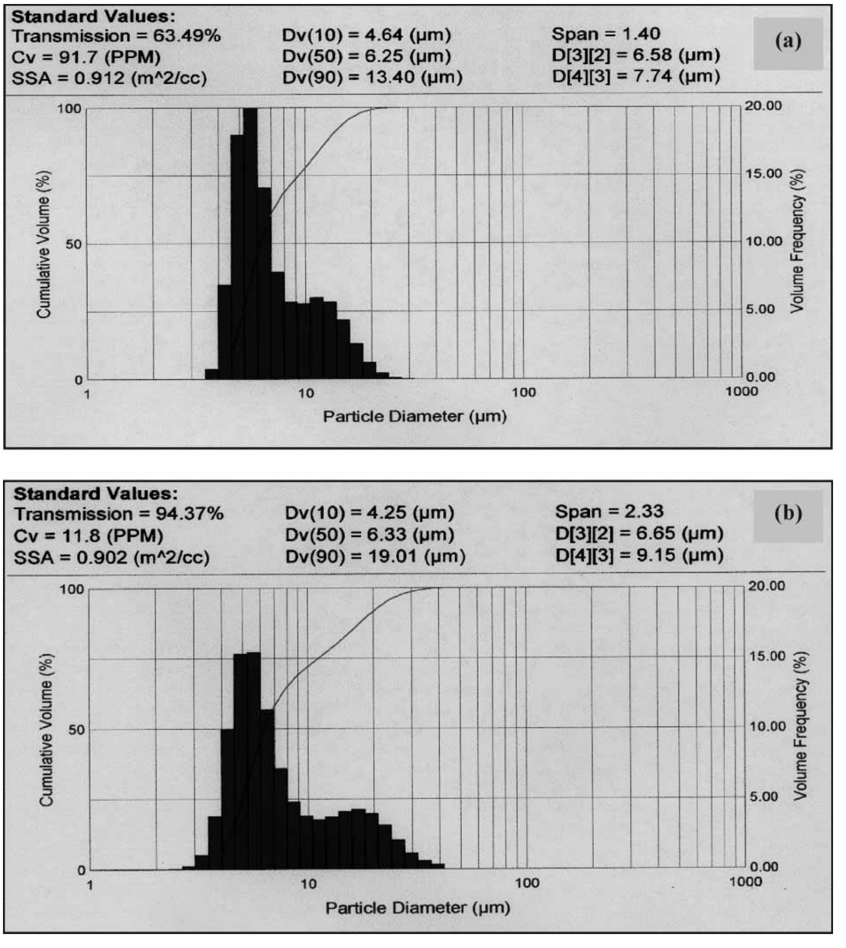


***Figure 6.*** Droplet size distribution for Reynolds number of 1350. (a) Voltage = 0.0 kV and initial droplet concentration = 12.1 $g/m^3$; (b) Voltage = 26 kV and droplet concentration = 5.96 $g/m^3$.

Droplet agglomeration continues in the column due to the electric field, leading to more effective removal of droplets.

## Light Transmission Profiles Along the Column

A number of experiments were carried out to investigate the effect of applied voltage on the light transmission profile along the column using a constant flow rate. The results of this experiment are shown in Fig. 7. This behavior

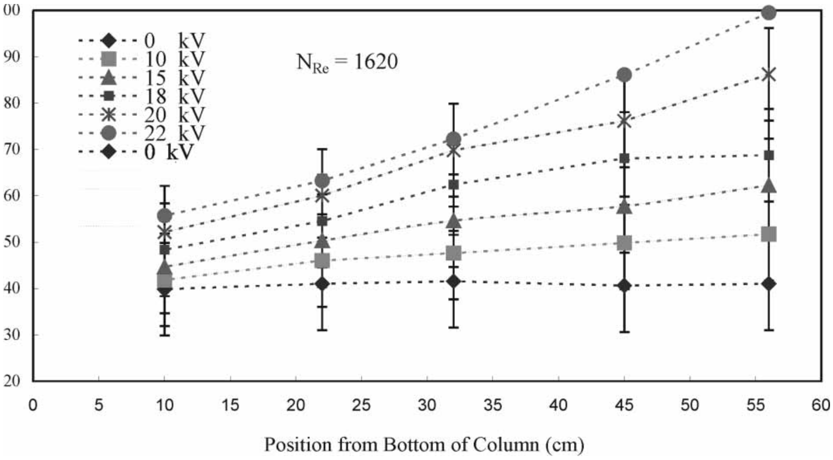


***Figure 7.*** Percent light transmission vs. height of column at Reynolds number of 1620 and inlet mist concentration of $27.3\,g/m^3$.



may be explained as follows. Transmission was essentially constant with no applied voltage, while light transmission increased with distance along the duct at greater values of applied voltage. The standard deviation for all experimental data obtained from repeated experiments is shown in the form of error bars. A large error bar indicates poor repeatability of the experiments, which may be attributed to a number of factors, including heat generated in the medium. This heat generation results in local temperature gradients, which, in turn, gives rise to gradients in the conductivity and permittivity of the medium. This effect can induce unwanted fluid movements that cause errors in measured data. Another reason could be the collision of the droplets on the laser observation window, which causes moisture to appear on the window and thereby results in inaccurate measurement.

## Multiple Mist Densities at Constant Flow Rates

A number of experiments were carried out to better understand the influence of electric field on initial droplet concentration at a constant flow rate. In this regard, three different initial droplet concentrations were used under a variable electric field that changed from 0 to 28 kV. The results of these experiments are shown in Fig. 8. As seen in the figure, as the voltage increases, the droplet concentrations uniformly decrease from the three different starting levels and approach the same value. This behavior may be caused by the buildup and re-entrainment of water droplets from the surface of the electrodes. It should be noted here that these measurements are only drop

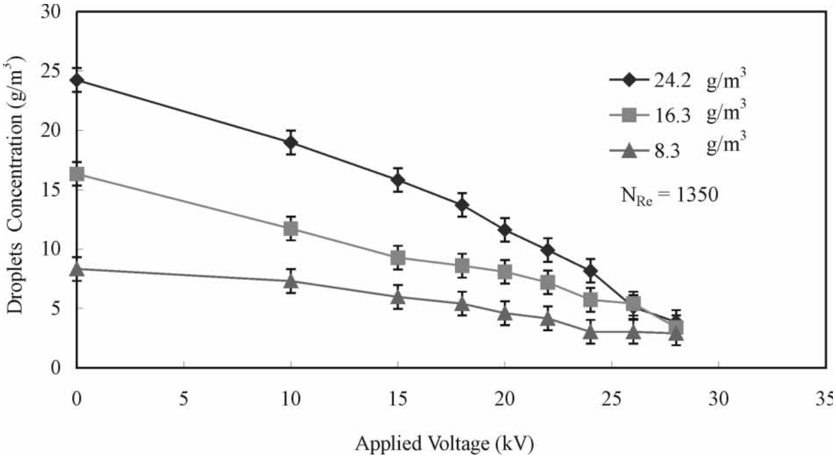


***Figure 8.*** Collected droplets in outlet gas stream vs. applied voltage at Reynolds number of 1350.



concentrations since the humidity at the exit of the sampling stream has already been subtracted.

## Constant Initial Mist Concentration

Experiments were conducted to investigate the effect of variable flow rate on droplet concentration under various electric field strengths. In each set of experiments, the starting droplet concentration was the same. The results of these experiments for a starting droplet concentration of $14.5\,g/m^3$ and Reynolds numbers of 940, 1350, and 1680 are shown in Fig. 9. As seen in the figure, the droplet concentration uniformly reduces with voltage to a certain value. However, after this point, further increases in the voltage no longer change the droplet concentration. This appears to be due to charge saturation.

## Removal Efficiency of Droplets

A key objective of this research was to quantify the removal efficiency of droplets from an air stream at constant flow rates under a dc electric field. To achieve this objective, several experiments were carried out. In this regard, three different droplet concentrations were used under a variable electric field that changed from 0 to 28 kV. The results of these experiments are shown in Fig. 10, which reveals that the removal efficiency of all three

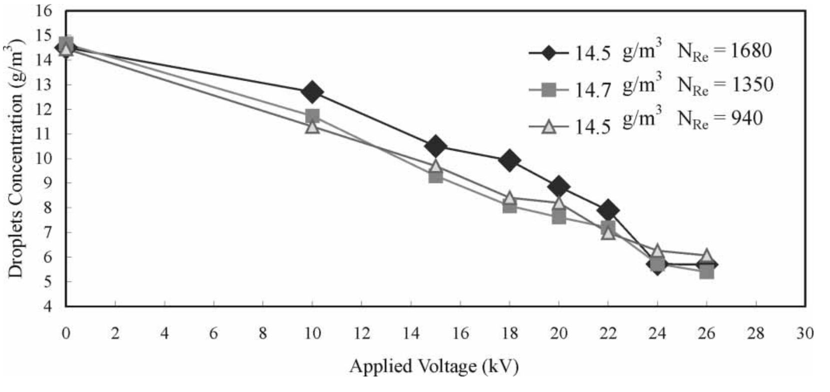


***Figure 9.*** Collected droplet in outlet gas vs. applied voltage at Reynolds numbers of 940, 1350, and 1680.



droplet concentrations varies approximately linearly with the applied voltage. At a droplet concentration of $8.3\,g/m^3$, saturation occurred at electric fields above $3.0-3.5\,kV/cm$ and the removal efficiency was steady at 63.5%. At droplet concentrations of 24.2 and $16.3\,g/m^3$, the removal efficiencies were 84.0 and 79.0%, respectively. Comparing the plots, we can conclude that the higher droplet concentration gives higher removal efficiency, presumably due to a larger number of droplet collisions.

## SUMMARY AND CONCLUSIONS

A series of experiments were conducted in a carefully designed duct in order to quantify the effect of an applied electric potential on the reduction

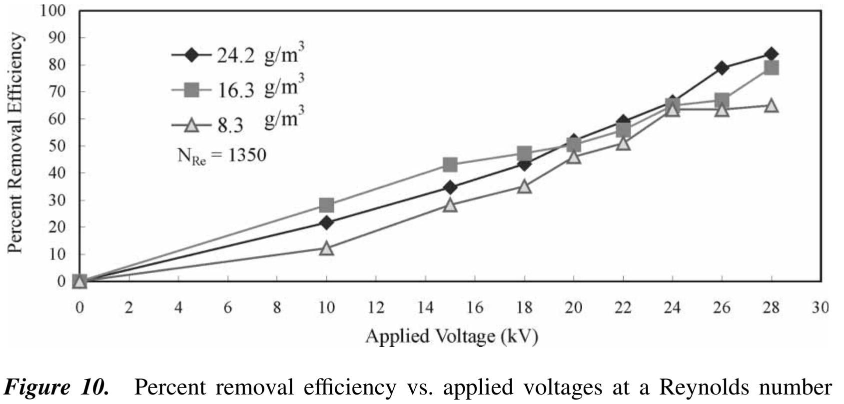


***Figure 10.*** Percent removal efficiency vs. applied voltages at a Reynolds number of 1350.

of water droplet content in simulated moist air streams. Analysis of the data showed that the water droplets in the mist ranged in diameter from a few micrometers to about 20 μm, more or less, in each of the test experiments. The droplet loadings in the inlet air streams, determined by freezing samples withdrawn isokinetically, ranged from nominal values of 8 to $24\,g/m^3$. The following conclusions are drawn from experimental results and observations:

1. In all but one of the cases investigated, the applied electric potentials reduced the mist content of the air exiting the test unit as the potential was increased from 0 to 28 kV. In that particular case, there was no further reduction in water droplet content of the air stream when the potential was increased from 24 to 28 kV, suggesting that a saturation effect may be occurring.
2. The efficiency of the droplet removal process ranges from about 65 to 85% on a mass basis for the series of runs at nominal Reynolds numbers of 1350, with the higher efficiencies corresponding to the higher nominal initial droplet loading of $24\,g/m^3$. The removal efficiency of 65% was achieved for a nominal droplet loading of $8\,g/m^3$.
3. In a strict sense, the effect of the applied electric potential on the water droplet content of the air stream is not linear. However, fitting the data with a linear model may be useful for preliminary engineering design purposes.
4. The water droplets migrate to the electrodes when the electric potential is applied across the plates, as evidenced by water accumulation on the plate surfaces. Although not quantified, it appeared that more water accumulated on the positive electrode than on the negative one. Accumulation of mist on the plates results in draining of water down the plates and pooling at the bottom of the unit. Mist begins to form near the bottom of the electrode plates and progresses in time up the plates. This migration of mist from the air stream to the plates due to the influence of the electric potential is the principal mechanism of droplet removal from the air stream in these experiments.
5. Experiments show that the droplet content of the air stream decreases approximately linearly with the distance up the test unit. This result suggests that further increases in removal efficiencies can be achieved by the use of electrode plates longer than the 60 cm used in these experiments.
6. There is limited evidence that the electric potential promotes droplet coalescence in the size range of approximately 10 to 20 μm. This process should improve droplet collection efficiency in a filter installed downstream of an electric potential demisting unit in an actual application, although sufficient data are not provided here to quantify the extent to which the overall droplet collection efficiency may be improved.

## REFERENCES

1. Brown, R.C. (1981) Capture of Dust Particles in Filters by Line-Dipole Charged Filters. *J. Aerosol Sci.*, 12: 349.
2. Davies, R.N. (1953) Dust is Dangerous; London: Faker & Faker Limited.
3. Cadle, R.D. (1965) Particle Size. Theory and Industrial Applications; New York: Reinhold Publishing Corporation.
4. Kildes, J., Bhatia, V., Lind, L., Johnson, E., and Johansen, A. (1995) An Experimental Investigation for Agglomeration of Aerosols in Alternating Electric Fields. *Aerosol Sci. Technol.*, 23: 603–610.
5. Barker, R.E., Brunson, R.R., Clinton, S.D., and Watson, J.S. (1991) Granular Electrofiltration. *Sep. Technol.*, 1 (3): 166–174.
6. Fuchs, N.A. (1964) Mechanics of Aerosols; New York: Pergamon.
7. Loffler, F. and Gutsch, A.J. (1993) Electrically Induced Aerosol Agglomeration: Formulation of the Collision Frequency and Simulating Agglomerate Growth. *J. Aerosol Sci.*, 24: S505–S506.
8. Zhang, X., Basaran, O.A., and Wham, R.M. (1995) Theoretical Prediction of Electric Field-Enhanced Coalescence of Spherical Drops. *AIChE J.*, 41: 1629.
9. Luckner, J., Wertejuk, Z., and Gradon, L. (1995) Experimental Studies of the Fibrous Filters Coupled with External Electrical Field. *J. Aerosol Sci.*, 26: S915–S916.
10. Barker, R.E. (1988) Granular Electrofiltration; Ph.D. Dissertation, University of Tennessee, 8–21.
11. Silverman, L., Billings, C.E., and Dennis, R. (1954) Performance of the Model K Electro-polar Filter; USAEC Report NYO 1592, Cambridge, Massachusetts: Harvard University.
12. Harriott, G.M. and Saville, D.A. (1971) Electrically Stimulated Aerosol Filtration in Packed Beds. *AIChE J.*, 26: 325.
13. Waterman, L.C. (1965) Electrical Coalescers. *Chem. Eng. Prog.*, 61: 51–57.
14. Thomas, J.W. and Woodfin, E.J. (1959) Electrified Fibrous Air Filter. *AIEE Trans.*, 78: 276.
15. Bogardus, H.F., Clark, R.C., Thompson, J.K., and Fielding, G.H. Enhancement of Filter Media Performance by Corona-Free Electric Fields. Presented at the 13th AEC Air Cleaning Conference, August 1974.
16. Fielding, G.H., Bogardus, H.F., Clark, R.C., and Thompson, J.K. (1975) Electrically Augmented Filtration of Aerosols. *ACS Symp. Ser.*, 17: 68–78.
17. Henry, F.S. and Ariman, T. (1986) Numeric Modeling of Electrically Enhanced Fibrous Filtration. Fluid Filtration. *Gas*; ASTM Committee F-21, American Society for Testing and Materials: Philadelphia, PA, 13–26.
18. Accomazzo, M.A. and Grant, D.C. (1986) Mechanisms and Devices for Filtration of Critical Process Gases. Fluid Filtration: Gas. ASTM STP 975, American Society for Testing and Materials: West Conshohocken, Pennsylvania, 402.
19. Riahi-Nezhad, C.K. (2001) The Effect of Electric Field on Moving Aqueous Aerosol Suspended in a Dynamic Fluid Chamber; M.S Thesis, University of Tennessee, 27–32.